Phase-sensitive spectroscopy of surface plasmons in individual metal nanostructures

A. A. Mikhailovsky,[1,*] M. A. Petruska,[1] Kuiru Li,[2] M. I. Stockman,[2,†] and V. I. Klimov[1,‡]
[1]*Chemistry Division, C-PCS, Los Alamos National Laboratory, Los Alamos, New Mexico 87545, USA*
[2]*Department of Physics and Astronomy, Georgia State University, Atlanta, Georgia 30303, USA*
(Received 7 July 2003; revised manuscript received 8 September 2003; published 6 February 2004)

We analyze both theoretically and experimentally the response of individual gold nanoparticles and nanoparticle dimers to a near-field excitation with broad-band radiation (a femtosecond white-light continuum) delivered through a subwavelength aperture. Because of the coherent superposition of the field emitted by the aperture and the secondary field reemitted by the nanostructure, the signals detected in the far zone exhibit a pronounced dependence on the phase of plasmon oscillations excited in the nanostructure. This phase sensitivity allows us to accurately determine positions of plasmon resonances not distorted by dielectric losses in a metal. In the near-field extinction spectra of individual nanoparticles, the plasmon resonance is observed as the ''zero-extinction'' point in which the transition from constructive (lower spectral energies) to destructive (higher spectral energies) interference occurs. By using spatially selective near-field excitation with a femtosecond white-light continuum, we are able to detect slight asymmetries in dimers composed of nominally identical nanoparticles.

DOI: 10.1103/PhysRevB.69.085401 PACS number(s): 68.37.Uv, 73.20.Mf, 78.67.−n, 85.35.−p

Optical responses of metal nanostructures can be manipulated via morphology-controlled resonances associated with surface plasmon (SP) modes.[1–3] These SP resonances lead to a significant enhancement of local electric fields, which can result in increased radiative decay,[4] large nonlinear-optical responses,[5] and strongly enhanced Raman scattering.[6–9] Near-field SP-enhanced interactions[10] also provide exciting opportunities for confining, guiding, and switching light using nanoscale, metal-based circuits (''SP nanophotonics'').[11,12]

Among the spectral and spatial properties of the SPs on the nanoscale, the phase (ϕ) of SP oscillations is one of the most important characteristics. In particular, if the SP phase spectrum is known, the condition $\phi=\pi/2$ determines the precise SP resonance frequency that is not affected by dielectric losses in the nanosystem. Therefore, the phase spectra can provide more accurate information on SP energies than the traditional intensity spectra. Furthermore, the manipulation of SP phases can allow one to control the spatial distribution of plasmon modes in metal nanostrucutres.[13]

In the case of macroscopic nanostructured samples (e.g., an ensemble of a large number of metal nanoparticles), the phase information can be lost in the integral signal because of the inevitable sample heterogeneities. A possible approach to experimentally detecting local phase responses is through the use of near-field measurements in which individual nanostructures can be spatially selected using a subwavelength aperture positioned in close proximity (<10 nm) to the sample surface.[14,15] The feasibility of imaging in the phase-sensitive regime has been demonstrated using a single wavelength excitation source and an external interferometer.[16,17] However, spectroscopic studies of the phase responses of individual nanostructures have not been conducted yet, likely because of the experimental difficulties associated with attaining broad-band, near-field illumination of a sufficiently high intensity.

In this article, we experimentally realize broad-band, phase-sensitive, nanoscale spectroscopy by using a femtosecond white-light continuum coupled into a fiber probe of a near-field scanning optical microscope (NSOM). We apply this broad-band, near-field spectroscopy to studies of individual gold nanoparticles and two particle aggregates (dimers). We observe that because of the coherent superposition of the aperture field and the secondary field reemitted by a nanostructure, the detected far-field spectra exhibit clear signatures of constructive and destructive interference and provide direct information regarding the phase of single-nanostructure plasmon oscillations. The analysis of these ''local'' interference spectra allows us to determine the frequencies and damping constants of plasmon resonances in individual nanoparticles. Furthermore, by using spatially selective, near-field excitation, we are able to detect slight asymmetries in dimeric systems comprising nominally identical nanoparticles. Our experimental findings are in agreement with the results of the semiquantitative modeling of near-field optical responses for both single particles and two-particle aggregates.

In our theoretical modeling, we consider a system of gold nanospheres of radii R_a ($a=1,2,\ldots$) subjected to the field $\mathbf{E}^A(\mathbf{r})$ of a nanoaperture of radius R_h in an ideal metal. The aperture field is described by the Bethe-Bouwkamp (BB) model;[18,19] we assume that the external excitation electric field is linearly polarized in the plane of the aperture (the x direction) and is of amplitude unity. At an ath nanosphere, this field induces multipole moments

$$q_{lm}^{(a)}=R_a^{l+2}\alpha_l E_{lm}^{(a)},\quad E_{lm}^{(a)}=\frac{2l+1}{4\pi}\int E_r^A(\mathbf{r})Y_{lm}^*(\theta,\varphi)d\Omega, \tag{1}$$

where the integral is extended over the surface of the nanosphere, $E_{lm}^{(a)}$ is the spherical tensor of the excitation field, $E_r^A(\mathbf{r})$ is the radial component of the aperture field at the nanosphere surface, $\alpha_l=[\varepsilon(\omega)-1]/[l\varepsilon(\omega)+l+1]$ is the dimensionless l-multipolar polarizability, and $\varepsilon(\omega)$ is the relative dielectric function of the nanosphere material at light

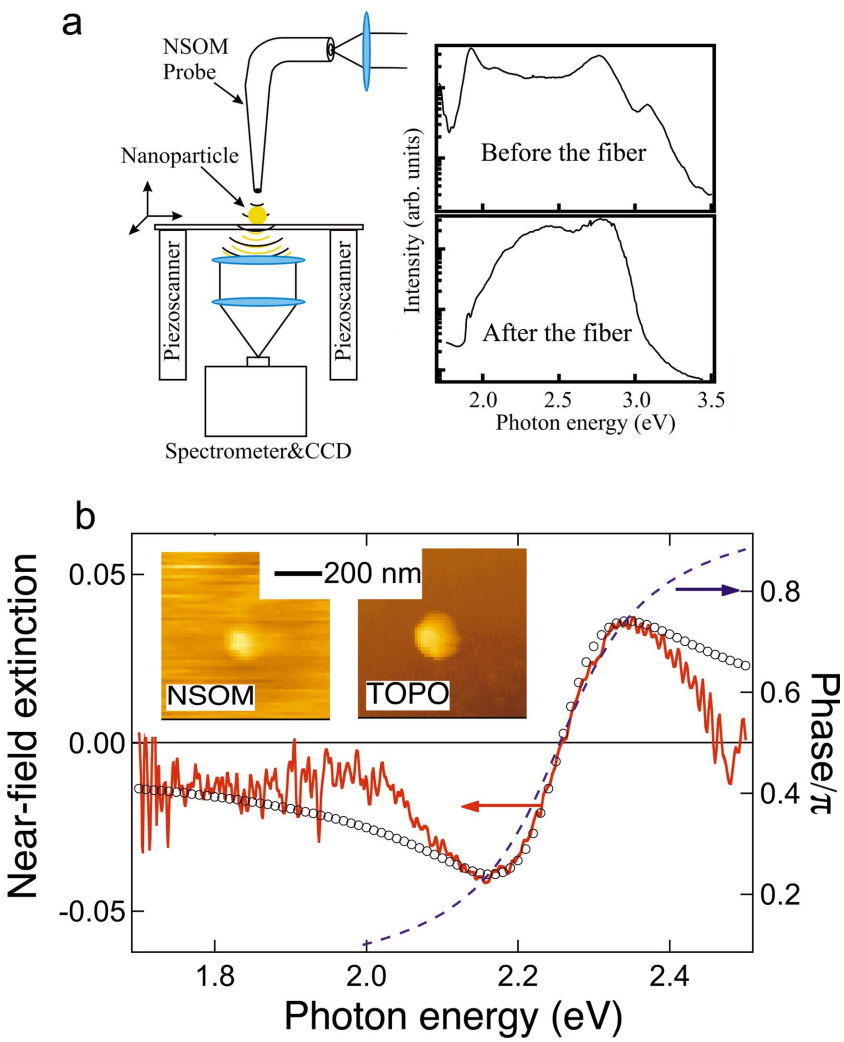

FIG. 1. (Color) (a) Illustration of near-field extinction measurements using broad-band illumination with a femtosecond white-light continuum (left); the spectra of the femtosecond continuum before and after the NSOM probe (right). (b) The near-field extinction spectrum (solid line) measured for an individual gold nanoparticle (nominally, $R=25$ nm) in comparison with the interference spectrum (open circles) calculated using Eqs. (3) and (5). The extracted SP phase spectrum is shown by the dashed line. Inset: topographic and near-field images of the nanoparticle. While the particle nominal size (diameter) is 50 nm, the "visible" size is larger because of resolution limitations of the NSOM.

frequency ω. Using $q_{lm}^{(a)}$ from Eq. (1) as the right-hand-side values in the coupled multipole equations,[20] we obtain the induced dipole moments of the nanospheres, which are further used to calculate the electric dipole ($E1$) radiation of the system in the far zone. In our semiquantitative modeling, we neglect the influence of the field of the particles on the aperture field, assuming that the metal surrounding the nanoaperture (in our experiments it is aluminum; see below) does not have plasmon resonances in the spectral range of the SP resonances of the gold nanospheres.

A nanohole in a perfect metal described by the BB model emits pure magnetic dipole ($M1$) radiation in the far zone.[18] However, the $M1$ and $E1$ radiations do not interfere efficiently because of the $\pi/2$ phase shift between them. Therefore, a relatively small $E1$ "leakage" from the tip covered by a "real" metal can significantly change the interference between fields emitted by the tip and the nanostructure. Importantly, this change modifies not only the radiation angular distribution but also the total flux, i.e., the observed extinction. As shown below, it can lead to the enhanced total transmission (the "nanoantenna" effect) in the spectral region immediately to the red of the SP resonance. Counterintuitively, this enhancement occurs despite strong dissipation in metal nanoparticles in the SP spectral region.

We will describe the $E1$ radiation of the near-field tip as that of an effective dielectric sphere with radius $R_s (R_s \leqslant R_h)$ and polarizability $R_s^3 \alpha_s$. This sphere is positioned at the center of the nanoaperture and emulates the dielectric core of the NSOM fiber tip. In the far zone, the $E1$ radiation of this effective sphere interferes with the $E1$ radiation of the metal nanoparticles and the $M1$ radiation of the nanoaperture to produce the resulting field that determines the intensity of the far-field signal. For the system of metal nanoparticles, we determine the near-field transmission $T=I/I_0$ and extinction $Q=-\ln(T)$, where I and I_0 are far-field intensities calculated in the presence and in the absence of nanoparticles, respectively.

First, we consider the case of a single gold nanoparticle (radius R and polarizability α) that is positioned at the axis of symmetry of the nanoaperture. For the collection solid angle of 2π, we obtain

$$T=1+A\cos\phi+B\sin\phi+C, \tag{2}$$

$$A=18\pi^2 k E_{sx} R_s^3 \alpha_s |\alpha| D, \quad B=64 R_h^2 |\alpha| D,$$

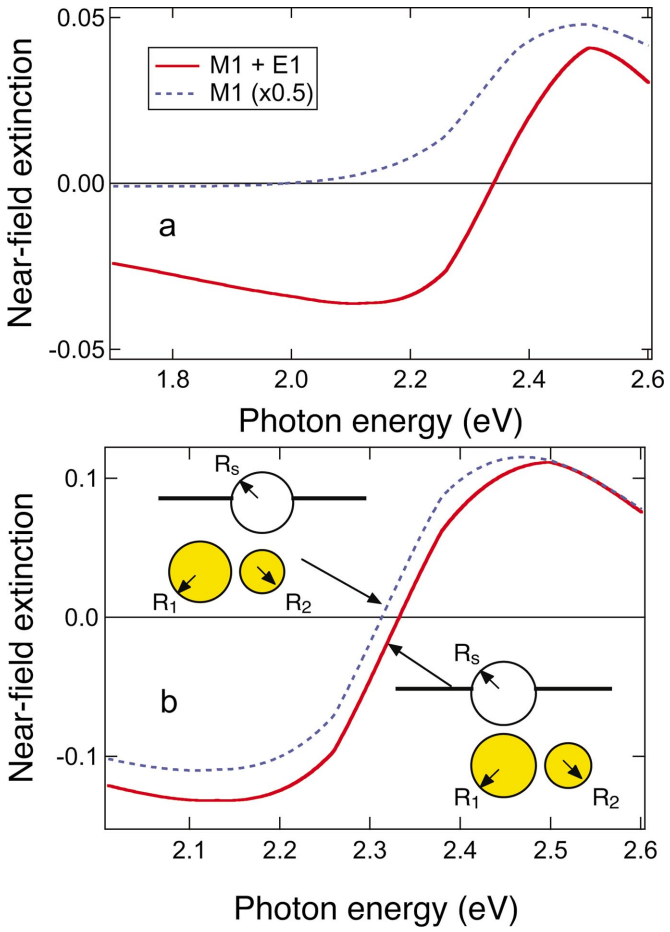

FIG. 2. (Color) (a) The near-field extinction spectra of an individual gold nanoparticle ($R=25$ nm) calculated using Eqs. (1)–(4) for two cases: the NSOM aperture is the purely $M1$ emitter ($R_s=0$) (dashed line; scaled by a factor of 0.5), and the aperture radiation contains both the $M1$ and $E1$ components ($R_s=30$ nm) (solid line); the aperture radius $R_h=30$ nm. (b) The calculated extinction spectra of the asymmetric dimer illuminated with unpolarized light through the near-field aperture located directly above either one or the other particle (insets); the dimer consists of particles of radii $R_1=28$ nm and $R_2=23$ nm separated by 2 nm (surface to surface). Nearly the same results are obtained for the linear polarization of the nanoaperture field oriented at $\pi/4$ with respect to the dimer axis.

$$C=9\pi^2 kE_x R^3|\alpha|^2 D, \quad D=\frac{kR^3E_x}{16R_h^4+9\pi^2k^2E_x^2R_s^6\alpha_s^2}.$$

Here E_{sx} and E_x are the x components of the effective field obtained from Eq. (1) ($l=1$) at the locations of the effective dielectric sphere and the metal nanoparticle, respectively, k is the radiation wave vector, and $\phi=\arg(\alpha)$ is the relative phase of the SP oscillations. Coefficients A and B describe the interference of the radiation of the metal nanoparticle with the $E1$ and $M1$ components of the tip emission, respectively, and C is a direct contribution from the radiation of the metal nanoparticle.

We assume that the emission of the tip is much stronger than that of a metal nanosphere $C \ll G \ll 1$, where $G=\sqrt{A^2+B^2}$. In this case, the modulation of the outgoing radiation by the nanosphere is weak, and we can present the local extinction and transmission as

$$Q=G\cos(\phi-\phi_0), \quad T=1+Q, \tag{3}$$

$$\phi_0=\arctan[32R_h^2/(9\pi^2kE_{sx}R_s^3\alpha_s)]. \tag{4}$$

The phase shift ϕ_0 is determined by the $E1$ and $M1$ radiations of the NSOM tip alone and is independent of the properties of the metal nanoparticle. Furthermore, ϕ_0 is a weak function of the frequency in the spectral range of SP resonances in gold particles and can be considered a constant. Hence, the near-field extinction spectrum [Eq. (3)] provides a direct measure of the phase spectrum of SPs.

If the SP resonance has a high finesse, i.e., the SP frequency ω_0 is much greater than its spectral width Γ, the phase spectrum has the same form as for a simple harmonic oscillator

$$\phi=\arccos[\Delta\omega/\sqrt{\Delta\omega^2+(\Gamma/2)^2}], \tag{5}$$

where $\Delta\omega=\omega-\omega_0$ is the detuning from the SP resonance. Thus, phase ϕ is equal to $\pi/2$ exactly at the resonance frequency ($\Delta\omega=0$), independent on the magnitude of Γ. Furthermore, if the constant phase shift ϕ_0 is small compared to $\pi/2$, the plasmon resonance is directly observable in the near-field extinction spectra as a zero-extinction point ($Q=0$), i.e., the point of crossover from negative (enhanced transmission) to positive (reduced transmission) extinction [Eq. (3)]. This effect is due to switching from constructive ($\omega<\omega_0$; in-phase SP oscillations) to destructive ($\omega>\omega_0$; out-of-phase SP oscillations) interference between the NSOM tip radiation and the induced field reemitted by a nanoparticle.

Experimentally, to measure single-particle extinction spectra, we use a NSOM [Fig. 1(a), left], in which the sample is illuminated through a ~50–100 nm aperture at the end of the Al-coated tapered fiber (the thickness of the coating is ~50 nm). Intense, broad-band, near-field illumination is provided by a femtosecond white-light continuum[21] generated by focusing 200-fs pulses from an amplified Ti-sapphire laser onto a sapphire plate. In addition to a wide spectral coverage [1.8 to 2.8 eV; Fig. 1(a), right] and a high brightness, the white-light continuum exhibits a low, laser-beam-like divergence, which allows us to couple it into a single-mode, near-field fiber with an efficiency greater than 40%.

We apply femtosecond white-light illumination for both imaging and spectroscopic measurements. In the imaging mode, the light transmitted through the sample is collected with a photomultiplier tube; in the spectroscopic mode, the transmitted light is dispersed in a spectrometer and is detected with a charge-coupled device (CCD). Simultaneously with the optical image, we obtain a topographic image using a feedback signal generated to maintain the constant tip-to-sample separation. The optical resolution in our measurements is defined by the aperture diameter and is ~50–100 nm.

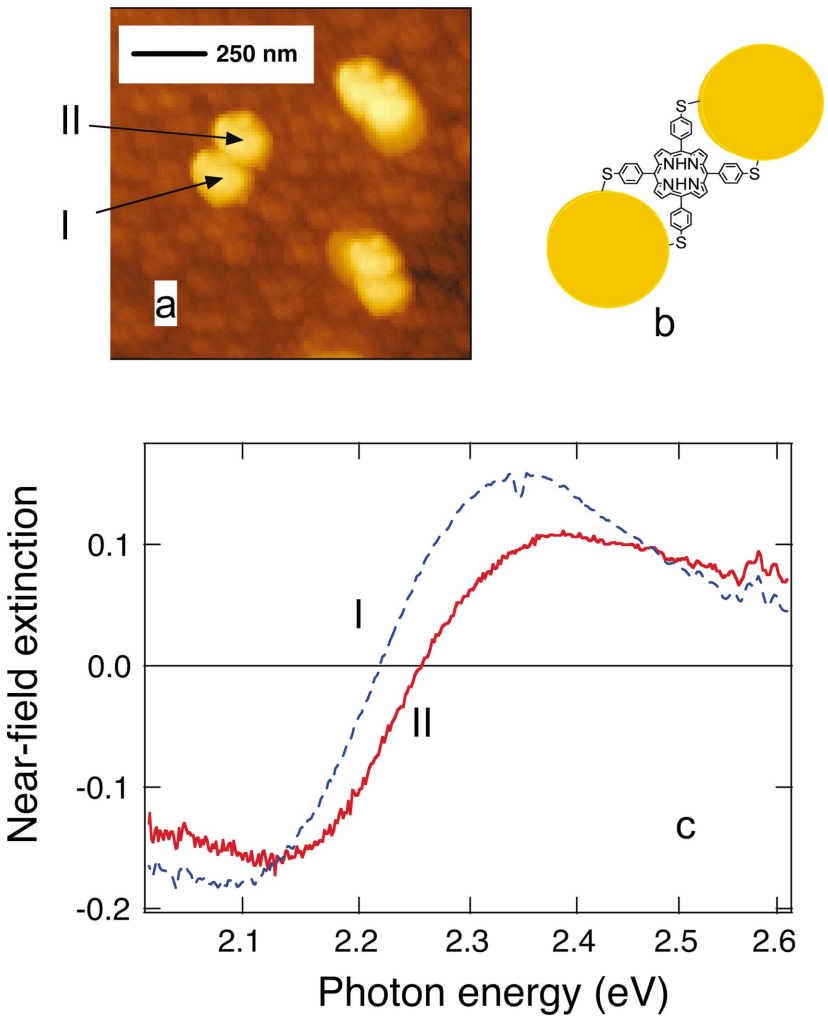

FIG. 3. (Color) (a) A topographic image of well-defined nanoparticle dimers molecularly engineered using the porphyrin linker illustrated in (b). (c) Two near-field spectra of an individual dimer measured by applying a driving field to either particle I or II [see panel (a)]; the NSOM probe was positioned using the optical images (not shown).

Samples of gold nanoparticles are prepared by allowing colloidal gold solutions to settle on thin layers of poly-*L*-lysine. In spectroscopic measurements, we acquire pairs of the transmitted light spectra by placing the near-field tip either directly above the selected nanoparticle $[I(\omega)]$ or above the nominally transparent substrate region $[I_0(\omega)]$. The recorded spectra are used to calculate the near-field extinction Q.

An example of the experimental spectrum recorded for a single particle with a nominal radius R of 25 nm is shown in Fig. 1(b) (solid line). It clearly exhibits the transition between destructive ($Q>0$) and constructive ($Q<0$) interference (the ''nanoantenna'' effect) predicted by our theoretical model. The theoretical spectrum calculated using Eqs. (1)–(4) taking into account both the $E1$ and $M1$ tip radiation ($R_h=R_s=30$ nm) [the solid line in Fig. 2(a)] closely reproduces both the magnitude and the overall spectral shape of the measured extinction, including the switching between negative and positive values of Q. Interestingly, in the spectrum calculated for the pure $M1$ emission of the aperture [the dashed line in Fig. 2(a)], the extinction is predominantly positive, indicating the importance of including in the model the $E1$ radiation of the tip. A small discrepancy (~ 0.1 eV) between the calculated and the experimental spectra in the position of the zero-extinction point is likely due to the fact that we approximate the nanoparticle polarizability by that of bulk gold.

To obtain further insight into the experimental spectra and to derive the positions and the widths of SP resonances, we treat ω_0, Γ, and ϕ_0 as adjustable parameters and apply a simple interference formula [Eq. (3)] in which both the relative phase ϕ [Eq. (5)] and the amplitude G are described by a forced harmonic oscillator model. By fitting the spectrum in Fig. 1(b) (open circles), we find $\omega_0=2.25$ eV, $\Gamma=180$ meV, and $\phi_0=0$. The fact that $\phi_0=0$ indicates that in our experiments the tip radiation is predominantly $E1$, and hence, the zero-extinction point indeed provides an accurate measure of the SP resonance not affected by dissipation in the metal. Furthermore, the calculated plasmon phase spectrum $\phi(\omega)$ [dashed line in Fig. 1(b)] indicates that the measured extinction closely correlates with the change in the phase that occurs around ω_0. The linewidth Γ derived from our near-field spectra is considerably smaller than that observed in ensemble spectra,[22] but it is comparable to the SP broadening measured in previous single particle studies.[23]

The near-field extinction spectra measured for particles of 10 and 5 nm radii (not shown) also indicate a clear transition from negative to positive extinction that occurs at 2.33 and

2.35 eV, respectively. These results indicate that the SP resonance frequency increases as the particle size is decreased, which is consistent with a trend observed in ensemble measurements.[22]

We have also applied our theory [Eqs. (1)–(4)] to near-field extinction spectra of two-particle aggregates (dimers) both consisting of identical and slightly different nanoparticles. In Fig. 2(b), we display the results for an asymmetric dimer of nanospheres whose radii differ by 5 nm (in these calculations we took into account the multipoles of up to the 30th order). We find a clear difference in the extinction spectra depending on whether the near-field driving ''force'' is applied to either the smaller (dashed line) or the larger (solid line) particle. This difference is due to the fact that the longitudinal SP mode in a dimer (the polarization oscillates along its axis) is red-shifted with respect to the SP frequency ω_0 in an isolated nanoparticle. This mode has a greater amplitude on the smaller nanosphere that plays the role of the dimer ''tip.'' In contrast, the twofold-degenerate transverse mode is blueshifted with respect to ω_0 and is localized preferentially on the larger nanosphere because of its higher polarizability. Therefore, the driving field applied to the smaller particle couples better to the longitudinal mode causing a low-energy shift of the extinction spectrum. The spectral shift is opposite if the larger particle is driven, which provides a better coupling to a high-energy transverse mode.

This result can be used for experimentally detecting slight asymmetries in a nanosystem, which can provide a much higher effective spatial resolution than the usual imaging mode. To illustrate this capability, we use our interference spectroscopy to detect small asymmetries in nominally symmetric dimers [Fig. 3(a)] engineered by covalently binding highly monodisperse ($\sim$10% size dispersion) gold nanoparticles of 25 nm mean radius with porphyrin linkers [Fig. 3(b)].[24] For a single dimer, we record two extinction spectra [Fig. 3(c)] by placing the NSOM tip above either one or the other nanoparticle [denoted by I and II in Fig. 3(a)]. We observe that the spectrum recorded by exciting particle I is redshifted with respect to that obtained when particle II is excited. This result indicates that the nominally symmetric dimer is actually built of nanoparticles that are of slightly different sizes. Furthermore, from our modeling [Fig. 2(b)] we can infer that particle I is smaller than II.

In conclusion, we have shown both theoretically and experimentally that the near-field extinction of metal nanoparticles is strongly affected by interference between the radiation of the near-field probe and the secondary field reemitted by the nanoparticle that acts as a nanoantenna, efficiently converting the near zone evanescent field into far-field radiation. We employ this effect to experimentally study SP resonances of individual gold nanoparticles and two-particle aggregates (dimers) using a high-intensity illumination with a broad-band, femtosecond white-light continuum coupled into a near-field fiber probe. We observe the pronounced signatures of the nanoantenna effect, in particular, a strong enhanced transmission (negative near-field extinction) in the spectral region immediately below the SP resonance, which is due to constructive interference between the radiations of the NSOM tip and the nanoparticle. The measured near-field interference spectra provide accurate information on the frequencies of SP resonances in individual nanoparticles not affected by dielectric losses and allow us to derive the SP linewidths and the phase spectra of SP oscillations. We also demonstrate that broad-band, near-field spectroscopic measurements can be used to detect slight asymmetries in nominally symmetric nanosystems (e.g., dimers) that are undetectable in the usual imaging mode.

This work was supported by Los Alamos LDRD Funds and the Chemical Sciences, Biosciences and Geosciences Division of the Office of Basic Energy Sciences,Office of Science, the U.S. Department of Energy. The authors thank Jennifer Hollingsworth for assistance with sample preparation and Anthony Burrell for synthesizing the porphyrin molecule used to prepare dimers.

*Present address: Department of Chemistry and Biochemistry, University of California, Santa Barbara, CA 93106.

†Electronic address: mstockman@gsu.edu; URL: http://www.phy-astr.gsu.edu/stockman

‡Author to whom correspondence should be addressed; electronic address: klimov@lanl.gov

[1] U. Kreibig and M. Vollmer, *Optical Properties of Metal Clusters* (Springer-Verlag, Berlin, 1995).

[2] H. Raether, *Surface Plasmons* (Springer-Verlag, Berlin, 1998).

[3] M.I. Stockman, S.V. Faleev, and D.J. Bergman, Phys. Rev. Lett. **87**, 167401 (2001).

[4] A.M. Glass, P.F. Liao, J.G. Bergman, and D.H. Olson, Opt. Lett. **5**, 368 (1980).

[5] R. Neuendorf, M. Quinten, and U. Kreibig, J. Chem. Phys. **104**, 6348 (1996).

[6] M.I. Stockman, V.M. Shalaev, M. Moskovits, R. Botet, and T.F. George, Phys. Rev. B **46**, 2821 (1992).

[7] K. Kneipp, Y. Wang, H. Kneipp, L.T. Perelman, I. Itzkan, R.R. Dasari, and M.S. Feld, Phys. Rev. Lett. **78**, 1667 (1997).

[8] S. Nie and S.R. Emory, Science **275**, 1102 (1997).

[9] A. Hartschuh, E.J. Sánchez, X.S. Xie, and L. Novotny, Phys. Rev. Lett. **90**, 095503 (2003).

[10] J.R. Krenn *et al.*, Phys. Rev. Lett. **82**, 2590 (1999).

[11] M.L.M. Balistreri, J.P. Korterik, L. Kuipers, and N.F. van Hulst, Phys. Rev. Lett. **85**, 294 (2000).

[12] S.I. Bozhevolnyi, V.S. Volkov, and K. Leosson, Phys. Rev. Lett. **89**, 186801 (2002).

[13] M.I. Stockman, S.V. Faleev, and D.J. Bergman, Phys. Rev. Lett. **88**, 067402 (2002).

[14] D.W. Pohl, W. Denk, and M. Lanz, Appl. Phys. Lett. **44**, 651 (1984).

[15] A. Harootunian, E. Betzig, M. Isaacson, and A. Lewis, Appl. Phys. Lett. **49**, 674 (1986).

[16] R. Hillenbrand and F. Keilmann, Appl. Phys. B: Lasers Opt. **73**, 239 (2001).

[17] M. Vaez-Iravani and R. Toledo-Crow, Appl. Phys. Lett. **62**, 1044 (1993).

[18] H.A. Bethe, Phys. Rev. **66**, 163 (1944).

[19] C.J. Bouwkamp, Philips Res. Rep. **5**, 321 (1950).
[20] J.M. Gérardy and M. Ausloos, Phys. Rev. B **22**, 4950 (1980).
[21] R.L. Fork, C.V. Shank, C. Hirlimann, and R. Yen, Opt. Lett. **8**, 1 (1983).
[22] S. Link and M.A. El-Sayed, J. Phys. Chem. B **103**, 4212 (1999).
[23] T. Klar, M. Perner, S. Grosse, G. von Plessen, W. Spirkl, and J. Feldmann, Phys. Rev. Lett. **80**, 4249 (1998).
[24] J.P. Novak and D.L. Feldheim, J. Am. Chem. Soc. **122**, 3979 (2000).